JPET #117184

**Title Page**

**Effects of the inducible nitric oxide synthase inhibitor L-N$^6$-(1-iminoethyl)-lysine on microcirculation and reactive nitrogen species generation in the kidney following lipopolysaccharide administration in mice.**

Liping Wu and Philip R. Mayeux

 Department of Pharmacology and Toxicology

University of Arkansas for Medical Sciences, Little Rock, AR 72205.

1

JPET #117184

**Running Title Page**

Running Title: RNS generation during LPS-induced renal injury

Corresponding Author: Philip R. Mayeux, Ph.D.

Department of Pharmacology and Toxicology

University of Arkansas for Medical Sciences

4301 West Markham Street, # 611

Little Rock, AR 72205

501-686-8895 501-686-5521 fax

prmayeux@uams.edu

Text pages    13
Tables        0
Figures       7
References  38
Words in the Abstract        243
Words in the Introduction  539
Words in the Discussion    964

ABBREVIATIONS:

RNS, reactive nitrogen species; ROS, reactive oxygen species; LPS, lipopolysaccharide; iNOS, inducible nitric-oxide synthase; DHR, dihydrorhodamine 123; RBC, red blood cell; IVVM, intravital videomicroscopy; L-NIL, L-$N^6$-(1-iminoethyl)-lysine; FITC-dextran, fluorescein isothiocyanate-dextran

Recommended assignment: Toxicology

## Abstract

The mortality rate for septic patients with acute renal failure is approximately doubled compared to patients with sepsis alone and unfortunately, the treatment for sepsis-induced renal failure has advanced little during the last several decades. Since sepsis is often caused by lipopolysaccharide (LPS), a mouse model of LPS challenge was used to study the development of kidney injury. We hypothesized that inducible nitric oxide synthase (iNOS)-catalyzed NO production and generation of reactive nitrogen species (RNS) might play a role in the microcirculatory defect and resulting tubular injury associated with LPS administration. Fluorescent intravital videomicroscopy was used to assess renal peritubular capillary perfusion and document RNS generation by renal tubules in real-time. As early as 6 h following LPS administration (10 mg/kg, i.p.) RNS generation (rhodamine fluorescence), redox stress (NAD(P)H autofluorescence), and the percentage of capillaries without flow were each significantly increased compared to saline-treated mice ($p < 0.05$). The generation of RNS was supported by the detection of nitrotyrosine-protein adducts in the kidney using immunohistochemistry. The iNOS inhibitor L-$N^6$-(1-iminoethyl)-lysine (L-NIL; 3 mg/kg, i.p.) completely blocked the increase in rhodamine fluorescence and NAD(P)H autofluorescence and prevented the capillary defects at 6 h following LPS administration. These results suggest that iNOS-derived RNS is an important contributor to the peritubular capillary perfusion defects and RNS generation that occur during sepsis and emphasize that pharmacological inhibition of iNOS may provided beneficial effects during sepsis by improving renal capillary perfusion and reducing RNS generation in the kidney.

3

## Introduction

Approximately 750,000 cases of sepsis are reported each year in the United States with an estimated cost incurred nationally at $17 billion annually (Dal Nogare, 1991). Acute renal failure (ARF) is a complication in approximately 20% - 50% of septic patients diagnosed by positive blood culture (Schrier and Wang, 2004) and the mortality rate for septic patients with ARF is approximately doubled compared to patients with sepsis alone (Angus and Wax, 2001). Therefore, renal failure is considered a critical prognostic factor in sepsis (Russell, 2006). Unfortunately, treatment of sepsis-induced ARF has advanced little during the last several decades (De Vriese and Bourgeois, 2003; Wan et al., 2003). Thus, a better understanding of the mechanism of kidney injury initiated by sepsis could lead to the uncovering of new therapeutic targets and more effective treatments for this serious condition.

Since sepsis is often caused by Gram-negative bacterial lipopolysaccharide (LPS), murine models of LPS challenge are frequently used to study the mechanisms of sepsis-induced renal failure. Studies suggest that the effects of LPS appear, at least in part, to be mediated by Toll-like receptor 4 (TLR4) and the initiation of the release of inflammatory cytokines such as TNFα (Cunningham et al., 2002; Cunningham et al., 2004). Notably, in septic patients with ARF, cytokine levels are positively correlated with mortality (Simmons et al., 2004) supporting the importance of the inflammatory response in the prognosis of sepsis-induced ARF. Moreover, the levels of circulating adhesion molecules are increased in the septic patient suggesting that vascular inflammation and endothelial activation may play a role in the development of organ

4

failure (Boldt et al., 1996). Cytokines and adhesion molecules are also elevated in the kidney following LPS challenge in the mouse, as is the generation of NO via another recognized inflammatory response, induction of inducible nitric oxide synthase (iNOS) (Cunningham et al., 2004; Guo et al., 2004; Wu et al., (in press)). Collectively, these inflammatory responses are likely contributors to renal injury during sepsis.

In models of ARF associated with iNOS induction, the contributions of reactive oxygen species (ROS) and reactive nitrogen species (RNS) are emerging as important mediators, particularly in ischemia/reperfusion injury (Noiri et al., 1996; Walker et al., 2000; Noiri et al., 2001; Vinas et al., 2006). Recent studies also suggest that iNOS-derived NO/RNS may play a role in the pathogenesis of LPS-induced renal injury (Wang et al., 2003; Cuzzocrea et al., 2006). However, the dynamics of RNS generation in the kidney has never been examined.

The development of sepsis-induced renal injury is a complex process. Recently, we reported that peritubular capillary perfusion is severely disrupted following LPS administration in mice (Tiwari et al., 2005; Wu et al., (in press)). Furthermore, this microcirculatory defect was positively correlated to the development of tubular cell stress (Wu et al., (in press)). The aim of the present study was to examine the relationship between the decrease in peritubular capillary perfusion and the generation of RNS. We utilized intravital videomicroscopy (IVVM) to monitor peritubular capillary perfusion and RNS generation following LPS administration. The iNOS inhibitor L-N$^6$-(1-iminoethyl)-lysine (L-NIL) was used to examine the role of iNOS. This study is the first to link early changes in renal microcirculation and tubular cell stress to iNOS-derived RNS generation by tubular epithelium.

**Methods**

Lipopolysaccharide (*E. coli* 055:B5 strain) and fluorescein isothiocyanate-dextran (FITC-dextran; 150,000 Da) were purchased from Sigma-Aldrich (St Louis, MO). Dihydrorhodamine 123 (DHR) was purchased from Invitrogen (Eugene, Oregon). Rabbit polyclonal anti-nitrotyrosine antibody was purchased from Upstate Cell Signaling Solutions (Lake Placid, NY). DakoCytomation LSAB® + System-HRP kit was purchased from Dako North America Inc. (Carpentaria, CA). L-N$^6$-(1-iminoethyl)-lysine·2HCl was purchased from Axxora (San Diego, CA).

*Mouse model of endotoxin-induced renal injury*

All animals were housed and killed in accordance with the National Institutes of Health Guide for the *Care and Use of Laboratory Animals* and with approval of the *University of Arkansas for Medical Sciences Institutional Animal Care and Use Committee*. Male C57BL/6 mice (8 weeks of age) were acclimated for 1 week with free access to food and water. At the start of the experiment mice were injected with saline or LPS (10 mg/kg, i.p.). At the indicated time after IVVM analysis, blood was collected via cardiac puncture under isoflurane anesthesia. This was followed immediately by cervical dislocation. Kidneys were then rapidly harvested and fixed in 10% phosphate-buffered formalin prior to embedding in paraffin. Serum creatinine concentration was determined using a Roche Cobas Mira Clinical Analyzer (Roche Diagnostic Systems, Inc., Branchburg, New Jersey).

*Evaluation of Peritubular Capillary Dysfunction with Intravital Videomicroscopy (IVVM)*

At 15 min prior to IVVM, mice were administered FITC-dextran (150,000 Da, 2 µmol/kg) and DHR (4 µmol/kg) via the tail vein. Mice were prepared for IVVM as

described elsewhere (Tiwari et al., 2005). Briefly, mice were anesthetized with isoflurane and underwent laparotomy to expose the left kidney. The kidney was positioned on a glass stage above an inverted fluorescent microscope (Zeiss Axiovert 200, Jena, Germany) equipped with a digitizing camera (Hamamatsu, Bridgewater, NJ) and kept moist with saline and covered. Core temperature was monitored and maintained at 36-37°C using an infrared heat lamp.

During IVVM the renal intravascular space and red blood cell (RBC) movement were visualized with FITC-dextran using an excitation of 470 nm and an emission of 520 nm. From the left kidney of each animal, videos of 10-sec each were captured at approximately 15 frames/sec from five randomly selected fields of view (200×). Capillary function was analyzed as previously described (Tiwari et al., 2005; Wu et al., (in press)). Briefly, randomly selected vessels (approximately 150 per kidney) were classified into three categories of blood perfusion: "Continuous Flow", where RBC movement in the vessel was not interrupted during the video; "Intermittent Flow", where RBC movement stopped or reversed any time during the video; and "No Flow", where no RBC movement was detected. Data were expressed as the percentage of vessels in each of the three categories.

*Evaluation of renal tubular epithelial cell stress using IVVM*

IVVM can be used to assess cellular redox stress by monitoring [NAD(P)H] autofluorescence (Paxian et al., 2004; Wunder et al., 2005). NAD(P)H autofluorescence was visualized at an excitation of 365 nm and an emission of 420 nm. To minimize photo bleaching, a <3-sec exposure was used to capture videos of five randomly selected fields of view per animal. Imaging settings were identical for all fields of view.

The intensity of NAD(P)H autofluorescence was quantified using AxioVision Imaging Software (Zeiss, Jena, Germany). Data were expressed as arbitrary units per $\mu m^2$.

*Detection of ROS/RNS using IVVM*

DHR is oxidized to fluorescent rhodamine by hydroxyl radical, nitrogen dioxide, peroxynitrite, and peroxidase-derived species (Halliwell and Whiteman, 2004). For each field of view captured for assessing capillary perfusion, additional images of rhodamine fluorescence were captured using an emission of 507 nm and an excitation of 530 nm. A <3-sec exposure was used to minimize photo bleaching. Imaging settings were identical for all fields of view. The intensity of rhodamine fluorescence was quantified using AxioVision Imaging Software (Zeiss, Jena, Germany). Data were expressed as arbitrary units per $\mu m^2$.

*Immunohistochemistry*

Immunohistochemistry was used to identify the presence of nitrotyrosine-protein adducts, a biomarker of peroxynitrite generation (Beckman et al., 1990). Paraffin-embedded sections (3 μm) from the right kidney (not used for IVVM) were cleared in xylene, and rehydrated with ethanol. Endogenous peroxidase activity and non-specific protein binding were blocked using reagents supplied in the DakoCytomation LSAB®+ System-HPR kit. Sections were incubated with rabbit anti-nitrotyrosine antibody (1:400 dilution) overnight at 4°C. Sections were then incubated with the second antibody (biotinylated link supplied by the kit) at room temperature for 30 min. Sections were incubated with streptavidin peroxidase for 30 min, washed with phosphate buffered saline, and stained with a chromagen solution supplied by the manufacturer. Gill's hematoxylin II was used as a counter-stain. To determine non-specific binding, anti-

nitrotyrosine was incubated with 3-nitrotyrosine (10 mM) for 1 h prior to use.

*Treatment with L-NIL*

The role of iNOS was examined using the iNOS inhibitor L-NIL (Moore et al., 1994). The dose of L-NIL (3 mg/kg, i.p.) was chosen based on our previous studies in the mouse and rat (Thompson et al., 1991; Zhang et al., 2000) and was administered at the same time as LPS.

*Statistical Analysis.*

Data were analyzed with Prism 4.0 software for Mac (GraphPad Software, San Diego, CA). Each "n" represents data or tissue obtained from one mouse. Data are expressed as means $\pm$ S.E.M. A one-way ANOVA followed by the Student-Newman-Keuls post test was used to determine differences between groups. A *p* value < 0.05 was considered significant.

## Results

### Real-time Generation of ROS/RNS in the Kidney Following LPS Administration

We recently reported that significant peritubular capillary dysfunction occurred at 2 h following LPS administration and that capillary dysfunction preceded tubular redox stress and renal failure (Wu et al., (in press)). To examine the time course of ROS/RNS generation, rhodamine fluorescence was monitored at 0 h (saline-treatment), 2 h, 6 h, 18 h, and 24 h following LPS administration. At 6 h rhodamine fluorescence was elevated approximately three-fold ($p < 0.05$ compared to saline) and remained elevated through 18 h (Fig. 1). Representative images of the kidney captured from saline and LPS-treated (18 h) mice are shown in Fig. 2. Capillary flow (visualized by FITC-dextran) and rhodamine fluorescence are shown for a saline-treated mouse (Fig. 2A and 2B) and an LPS-treated mouse at 18 h (Fig. 2C and 2D). These images show intense rhodamine fluorescence (ROS/RNS generation) in the kidney from the LPS-treated mouse. Tubules found in regions of decreased capillary perfusion, indicated by arrows in Fig. 2C, appeared to display the highest level of rhodamine fluorescence. Higher magnification images in Fig. 3A (FITC-dextran) and 3B (rhodamine) suggested that rhodamine fluorescence intensity was highest in tubules bordered by capillaries with compromised flow.

### Immunohistochemical Detection of Nitrotyrosine-protein Adducts

The increase in rhodamine fluorescence suggested that RNS might have been generated in the kidney. To help confirm the generation of the RNS peroxynitrite, immunohistochemistry was used to detect nitrotyrosine-protein adducts, a marker of peroxynitrite generation. Little positive staining was observed in kidney sections from

10

saline-treated mice (Fig. 4A). In contrast, kidney sections from LPS-treated mice at 18 h showed extensive positive staining for nitrotyrosine in tubules (Fig. 4B). A preincubation of the antibody with 10 mM 3-nitrotyrosine prevented staining (Fig. 4C), thus indicating that the antibody was specific for nitrotyrosine. These findings help to validate the IVVM findings that DHR can be used to detect RNS generation in real-time.

*Contribution of iNOS to capillary dysfunction, ROS/RNS generation, and cellular redox stress*

To examine the effects of iNOS inhibition on LPS-induced events that could lead to renal failure, mice were studied prior to renal failure. Three groups of mice were studied: Saline, LPS, and LPS + L-NIL. At 6 h after dosing, mice underwent IVVM with FITC-dextran and DHR. Peritubular capillary perfusion was severely compromised in mice treated with LPS (Fig. 5). The percentage of capillaries with continuous flow was decreased from 89 ± 4% in Saline (n = 6) to 43 ± 7% in LPS (n = 6; $p < 0.05$ compared to Saline). The percentage of capillaries with intermittent and no flow was increased from 6 ± 2% and 5 ± 2% in Saline, respectively to 43 ± 4% and 16 ± 4% in LPS, respectively ($p < 0.05$ for intermittent flow compared to Saline and $p < 0.05$ for no flow compared to Saline). Thus, all of the effects of LPS on peritubular capillary perfusion were completely blocked by L-NIL.

The effect of L-NIL treatment on LPS-induced ROS/RNS generation was determined using oxidation of DHR to rhodamine as in Fig. 2. Representative video images of rhodamine fluorescence from a saline-treated, LPS-treated (10 mg/kg, i.p.), and L-NIL (3 mg/kg, i.p.) + LPS-treated mouse captured at 6 h are shown in Fig. 6A-C respectively. LPS produced a significant ($p < 0.05$) increase in rhodamine fluorescence

intensity compared to Saline at 6 h (Fig. 6D). The increase in rhodamine fluorescence was completed blocked by L-NIL. Thus, the ability of L-NIL to block the increase in LPS-induced rhodamine fluorescence suggests that iNOS-derived RNS were the major oxidative species generated at 6 h following LPS treatment.

IVVM was also used to assess cellular redox stress by measuring NAD(P)H autofluorescence (Fig. 7). Representative video images of NAD(P)H autofluorescence from a saline-treated, LPS-treated (10 mg/kg, i.p.), and L-NIL (3 mg/kg, i.p.) + LPS-treated mouse captured at 6 h are shown in Fig. 7A-C respectively. LPS caused in a significant increase in NAD(P)H autofluorescence ($p < 0.05$ compared to Saline) that was completely blocked by co-administration of L-NIL (Fig. 7D).

Taken together, these results indicate that iNOS-derived NO mediates the decrease in capillary perfusion, RNS generation, and tubular redox stress associated with LPS administration.

## Discussion

It is becoming increasingly clear that endothelial injury and peritubular capillary dysfunction may initiate and extend the pathogenesis of chronic renal failure (O'Riordan et al., 2005) and also contribute to nephrotoxic and ischemic forms of acute renal failure (Brodsky et al., 2002; Yuan et al., 2003; Molitoris and Sutton, 2004) by compromising renal vascular responsiveness and tubule function (Linas and Repine, 1999; Piepot et al., 2003; O'Riordan et al., 2005). We have established that renal microcirculatory dysfunction is also a key feature of LPS-induced renal injury. Renal peritubular capillary perfusion is severely compromised as early as 2 h following LPS administration in mice and tubular redox stress increases as perfusion decreases (Wu et al., (in press)). In addition, induction of iNOS in the kidney parallels the time course of capillary dysfunction raising the possibility that increased NO generation may participate in the development of renal injury (Tiwari et al., 2005; Wu et al., (in press)). The present studies extend those studies to show the importance of iNOS in the early capillary defect. Furthermore, iNOS inhibition reduced tubular redox stress and blocked the increase in rhodamine fluorescence suggesting that the predominant oxidative species generated by the tubular epithelium in response to LPS were RNS.

Microcirculatory dysfunction is a common feature of several forms of renal injury. For example, IVVM has been used to document changes in peritubular capillary flow following renal ischemia (Sutton et al., 2005). However, the consequences of reduced peritubular capillary perfusion have never been studied in detail. IVVM is a powerful tool because it allows for real-time measurements of peritubular capillary perfusion and epithelial stress [NAD(P)H levels] and ROS/RNS generation in adjacent tubules. As

13

early as 6 h following LPS administration renal cortical RNS generation was significantly increased. Image analysis suggested that RNS generation was predominantly localized to the tubular epithelium and in particular, those tubules bordered by capillaries with compromised flow. These findings suggest that RNS generation by the tubular epithelium may be regulated by capillary perfusion. Thus, reduced peritubular capillary perfusion may contribute to tubular epithelial oxidant generation. These data are the first to show the association between decreased capillary perfusion and increased tubular RNS generation. A significant decrease in capillary perfusion occurs as early as 2 h following LPS administration (Wu et al., (in press)), preceding RNS generation. We also observed an early increase in tubular NAD(P)H levels, suggesting an increase in the redox state (Paxian et al., 2004; Wunder et al., 2005) of the tubular epithelium. The increase in NAD(P)H levels following LPS administration is a likely consequence of hypoxia caused by reduced capillary perfusion. For example, hepatic NAD(P)H levels are highly correlated with hypoxia in the liver (Paxian et al., 2004; Wunder et al., 2005). Thus, these data provide compelling evidence that localized decreases in peritubular capillary perfusion can result in a microenvironment that promotes oxidant generation and tubular injury. This type of cross-talk between the peritubular capillary and tubular epithelium may be important in other forms of renal injury as well.

Induction of iNOS results in overproduction of NO and increases the likelihood that RNS will be generated. NO reacts with superoxide to produce the RNS peroxynitrite, a highly reactive cytotoxic species (Szabo, 2003) that can be detected by DHR (Glebska and Koppenol, 2003). The finding that nitrotyrosine-protein adducts were present in the kidney following LPS administration indicated the generation of

peroxynitrite. Furthermore, those findings supported the interpretation of the IVVM experiments with DHR that RNS was generated by the renal tubules. While the precise source or superoxide is unknown, decreased capillary perfusion can lead to hypoxia and increased redox stress (Paxian et al., 2004; Wu et al., (in press)), both of which can result in increased superoxide generation. This raises the possibility that compromised capillary perfusion could lead to ROS/RNS generation.

We reported previously that pharmacological inhibition of iNOS could achieve full protection in mice against LPS-induced peritubular capillary dysfunction and renal failure at 18 h (Tiwari et al., 2005). In the present study we observed that L-NIL treatment prevented not only the early perfusion defects at 6 h but also prevented RNS generation and tubular redox stress. It is generally agreed that iNOS induction and the resulting overproduction of NO plays an important role in the hemodynamic changes associated with sepsis and sepsis-induced renal failure (Schrier and Wang, 2004). The kidney is somewhat unique in that LPS produces a paradoxical renal vasoconstriction (Lugon et al., 1989) thought to be due, at least in part, to iNOS-derived NO-mediated inactivation of eNOS (Schwartz et al., 1997; Chauhan et al., 2003). The present findings show that in addition to altering vascular reactivity, iNOS also serves as a major source of NO to generate RNS in kidney. Thus, these effects of NO could act synergistically to compromise renal function. Although these data provide compelling evidence for the role of iNOS, additional studies are required to fully establish cause-effect relationships that may exist between iNOS-derived NO and the decrease in peritubular capillary perfusion.

A unique feature of IVVM when applied to the kidney is the ability to directly monitor the effects of capillary flow on neighboring tubules. By determining capillary perfusion, RNS generation, and cellular redox stress in the same fields of view, we were able to uncover a previously unrecognized role for the peritubular capillary in regulating RNS generation. This study is the first to visualized RNS generation by renal tubules in response to LPS challenge *in vivo*. The data suggest that decreased capillary perfusion sets up a microenvironment that may promote tubular RNS generation and cellular redox stress. Pharmacological inhibition of iNOS blocked the capillary perfusion defects, tubular RNS generation and tubular cellular stress. This dependence on iNOS supports the notion that iNOS should be further evaluated as a potential therapeutic target in sepsis-induced renal injury.

JPET #117184

## Acknowledgments

**References**

Angus DC and Wax RS (2001) Epidemiology of sepsis: an update. *Crit Care Med* 29:S109-116.

Beckman JS, Beckman TW, Chen J, Marshall PA and Freeman BA (1990) Apparent hydroxyl radical production by peroxynitrite: Implications for endothelial injury from nitric oxide and superoxide. *Proc Natl Acad Sci USA* 87:1620-1624.

Boldt J, Muller M, Kuhn D, Linke LC and Hempelmann G (1996) Circulating adhesion molecules in the critically ill: a comparison between trauma and sepsis patients. *Intensive Care Med* 22:122-128.

Brodsky SV, Yamamoto T, Tada T, Kim B, Chen J, Kajiya F and Goligorsky MS (2002) Endothelial dysfunction in ischemic acute renal failure: rescue by transplanted endothelial cells. *Am J Physiol* 282:F1140-F1149.

Chauhan SD, Seggara G, Vo PA, Macallister RJ, Hobbs AJ and Ahluwalia A (2003) Protection against lipopolysaccharide-induced endothelial dysfunction in resistance and conduit vasculature of iNOS knockout mice. *FASEB Journal* 17:773-775.

Cunningham PN, Dyanov HM, Park P, Wang J, Newell KA and Quigg RJ (2002) Acute renal failure in endotoxemia is caused by TNF acting directly on TNF receptor-1 in kidney. *Journal of Immunology* 168:5817-5823.

Cunningham PN, Wang Y, Guo R, He G and Quigg RJ (2004) Role of Toll-like receptor 4 in endotoxin-induced acute renal failure. *Journal of Immunology* 172:2629-2635.

Cuzzocrea S, Mazzon E, Di Paola R, Esposito E, Macarthur H, Matuschak GM and Salvemini D (2006) A role for nitric oxide-mediated peroxynitrite formation in a model of endotoxin-induced shock. *J Pharmacol Exp Ther* 319:73-81.

Dal Nogare AR (1991) Southwestern internal medicine conference: septic shock. *American Journal of the Medical Sciences* 302:50.

De Vriese AS and Bourgeois M (2003) Pharmacologic treatment of acute renal failure in sepsis. *Curr Opin Crit Care* 9:474-480.

Glebska J and Koppenol WH (2003) Peroxynitrite-mediated oxidation of dichlorodihydrofluorescein and dihydrorhodamine. *Free Rad Biol Med* 35:676-682.

Guo R, Wang Y, Minto AW, Quigg RJ and Cunningham PN (2004) Acute renal failure in endotoxemia is dependent on caspase activation. *Journal of the American Society of Nephrology* 15:3093-3102.

Halliwell B and Whiteman M (2004) Measuring reactive species and oxidative damage in vivo and in cell culture: how should you do it and what do the results mean? *Br J Pharmacol* 142:231-255.

Linas SL and Repine JE (1999) Endothelial cells regulate proximal tubule epithelial cell sodium transport. *Kidney Int* 55:1251-1258.

Lugon JR, Boim MA, Ramos OL, Ajzen H and Schor N (1989) Renal function and glomerular hemodynamics in male endotoxemic rats. *Kidney Int* 36:570-575.

Molitoris BA and Sutton TA (2004) Endothelial injury and dysfunction: role in the extension phase of acute renal failure. *Kidney Int* 66:496-499.

Moore WM, Webber RK, Jerome GM, Tjoeng FS, Misko TP and Currie MG (1994) L-N[6]-(1-Iminoethly)lysine: a selective inhibitor of inducible nitric oxide synthase. *J Med Chem* 37:3886-3888.

Noiri E, Nakao A, Uchida K, Tsukahara H, M O, Fujita T, Brodsky SV and Goligorsky MS (2001) Oxidative nitrosative stress in acute renal ischemia. *Am J Physiol* 281:F948-F957.

Noiri E, Peresleni T, Miller F and Goligorsky MS (1996) In vivo targeting of inducible NO synthase with oligodeoxynucleotides protects rat kidney against ischemia. *J Clin Invest* 97:2377-2383.

O'Riordan E, Chen J, Brodsky SV, Smirnova I, Li H and Goligorsky MS (2005) Endothelial cell dysfunction: The syndrome in making. *Kidney Int* 67:1654-1658.

Paxian M, Keller SA, Cross B, Huynh TT and Clemens MG (2004) High-resolution visualization of oxygen distribution in the liver in vivo. *Am J Physiol* 286:G37-G44.

Piepot HA, Groeneveld AB, van Lambalgen AA and Sipkema P (2003) Endotoxin impairs endothelium-dependent vasodilation more in the coronary and renal arteries than in other arteries of the rat. *J Surg Res* 110:413-418.

Russell JA (2006) Management of sepsis. *N Engl J Med* 355:1699-1713.

Schrier RW and Wang W (2004) Acute renal failure and sepsis. *N Engl J Med* 351:159-169.

Schwartz D, Mendonca M, Schwartz I, Xia Y, Satriano J, Wilson CB and Blantz RC (1997) Inhibition of constitutive nitric oxide synthase (NOS) by nitric oxide generated by inducible NOS after lipopolysaccharide administration provokes renal dysfunction in rats. *Journal of Clinical Investigation* 100:439-448.

Simmons EM, Himmelfarb J, Sezer MT, Chertow GM, Mehta RL, Paganini EP, Soroko S, Freedman S, Becker K, Spratt D, Shyr Y and Ikizler TA (2004) Plasma cytokine levels predict mortality in patients with acute renal failure. *Kidney International* 65:1357-1365.

Sutton TA, Kelly KJ, Mang HE, Plotkin Z, Sandoval RM and Dagher PC (2005) Minocycline reduces renal microvascular leakage in a rat model of ischemic renal injury. *Am J Physiol* 288:F91-F97.

Szabo C (2003) Multiple pathways of peroxynitrite cytotoxicity. *Toxicology Letters* 140-141:105-112.

Thompson NT, Bonser RW and Garland LG (1991) Receptor-coupled phospholipase D and its inhibition. *TiPS* 12:404-408.

Tiwari MM, Brock RW, Kaushal GP and Mayeux PR (2005) Disruption of renal peritubular blood flow in lipopolysaccharide-induced renal failure: role of nitric oxide and caspases. *Am J Physiol* 289:F1324-F1332.

Vinas JL, Sola A and Hotter G (2006) Mitochondrial NOS upregulation during renal I/R causes apoptosis in a peroxynitrite-dependent manner. *Kidney Int* 69:1403-1409.

Walker LM, Walker PD, Imam SZ, Ali SF and Mayeux PR (2000) Evidence for peroxynitrite formation in renal ischemia-reperfusion injury: studies with the

inducible nitric oxide synthase inhibitor L-N$^6$-(1-iminoethyl)-lysine. *J Pharmacol Exp Ther* 295:417-422.

Wan L, Bellomo R, Di Giantomasso D and Ronco C (2003) The pathogenesis of septic acute renal failure. *Curr Opin Crit Care* 9:496-502.

Wang W, Jittikanont S, Falk SA, Li P, Feng L, Gengaro PE, Poole BD, Bowler RP, Day BJ, Crapo JD and Schrier RW (2003) Interaction among nitric oxide, reactive oxygen species, and antioxidants during endotoxemia-related acute renal failure. *Am J Physiol* 284:F532-F537.

Wu L, Tiwari MM, Messer KJ, Holthoff JH, Gokden N, Brock RW and Mayeux PR ((in press)) Peritubular capillary dysfunction and renal tubular epithelial cell stress following lipopolysaccharide administration in mice. *Am J Physiol.*

Wunder C, Brock RW, Krug A, Roewer N and Eichelbronner O (2005) A remission spectroscopy system for in vivo monitoring of hemoglobin oxygen saturation in murine hepatic sinusoids, in early systemic inflammation. *Comp Hepatol* 4:doi:10.11 186/1476-5926-1474-1471.

Yuan HT, Li XZ, Pitera JE, Long DA and Woolf AS (2003) Peritubular capillary loss after mouse acute nephrotoxicity correlates with down-regulation of vascular endothelial growth factor-A and hypoxia-inducible factor-1 alpha. *Am J Pathol* 163:2289-2301.

Zhang C, Walker LM and Mayeux PR (2000) Role of nitric oxide in lipopolysaccharide-induced oxidant stress in the rat kidney. *Biochem Pharmacol* 59:203-209.

JPET #117184

**Footnotes:**

**Figure Legends**

**Fig. 1.** Time course of ROS/RNS generation in the kidney following LPS administration. Rhodamine fluorescence was used to estimate ROS/RNS generation at the indicated time following LPS administration (10 mg/kg, i.p.). Rhodamine fluorescence was significantly elevated at 6 h and 18 h following LPS administration. Data are mean ± S.E.M. (n = 5-6 animals per group). *P < 0.05 compared to time 0 (saline treatment).

**Fig. 2.** Representative images captured during IVVM following LPS administration. Shown are images captured from the same field of view from a Saline-treated mouse (A: capillary perfusion; B: rhodamine fluorescence) and an LPS-treated mouse (10 mg/kg, i.p.) at 18 h (C: capillary perfusion; D: rhodamine fluorescence). Arrows indicate capillaries with intermittent or no flow. Rhodamine fluorescence was increased in regions of compromised flow. Magnification 200 x.

**Fig. 3.** Relationship between capillary perfusion and ROS/RNS generation. Representative video images of capillary perfusion (A) and rhodamine fluorescence (B) from the same field of view captured from an LPS-treated mouse (10 mg/kg, i.p.) are shown. Capillary perfusion was visualized using FITC-dextran and arrows indicate capillaries with intermittent or no flow (A). Image of rhodamine fluorescence was pseudo-colored to reveal differences in pixel density (B). Regions boarded by dysfunctional capillaries displayed higher relative pixel intensities.

**Fig. 4.** Immunohistochemistry of nitrotyrosine-protein adducts in the kidney. Representative photographs from the kidney of a saline-treated (A) and LPS-treated (10

mg/kg, i.p.) (B and C) mouse 18 h following treatment are shown (representative of three animals per group). Positive staining, indicated by a brown color, was weak in saline-treated mice. In contrast, LPS treated mice displayed intense staining in the tubules. The specificity of the anti-nitrotyrosine antibody was confirmed by blocking antigen-binding sites with 10 mM 3-nitrotyrosine (C). Magnification 200x.

**Fig. 5**. Effect of L-NIL on LPS-induced disruption of renal peritubular capillary perfusion. At 6 h following LPS administration, the percentage of capillaries with continuous flow was significantly decreased (*$p < 0.05$ compared with Saline) while the percentage of capillaries with intermittent or no flow were significantly increased (*$p < 0.05$ compared with Saline). L-NIL treatment (3 mg/kg, i.p.) blocked the effects of LPS on capillary perfusion. Data are mean ± S.E.M. (n = 6).

**Fig. 6.** Effects of L-NIL on LPS-induced ROS/RNS generation in the kidney. Representative video images of rhodamine fluorescence from a saline-treated (A), LPS-treated (10 mg/kg, i.p.) (B), and L-NIL + LPS-treated mice (C) at 6 h are shown. LPS produced a significant increase in rhodamine fluorescence at 6 h indicating the generation of ROS/RNS (*$p < 0.05$ compared with Saline). Treatment with L-NIL (3 mg/kg, i.p.) blocked this effect of LPS. Data are mean ± S.E.M. (n = 6). Magnification 200x.
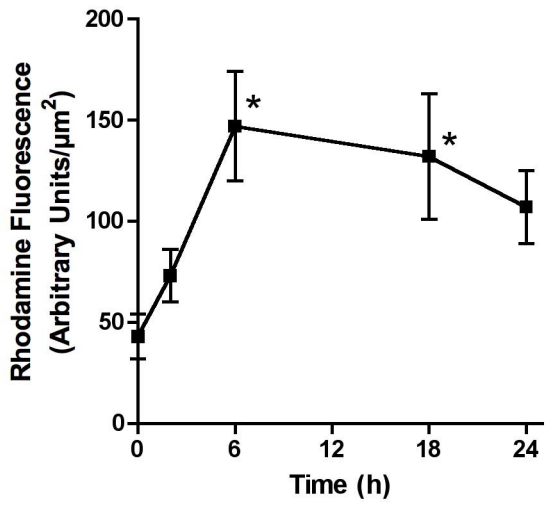
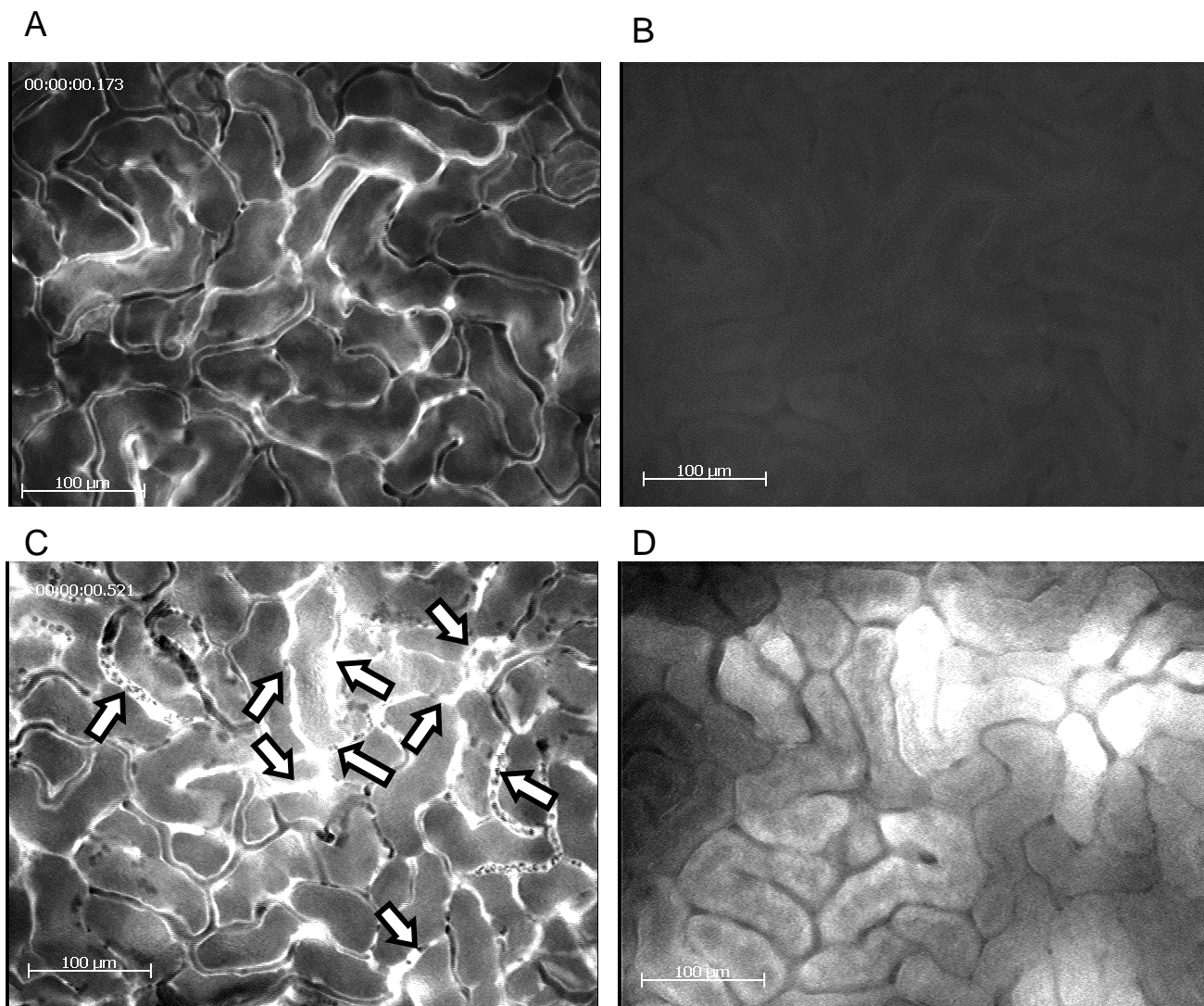**Fig. 7.** Effects of L-NIL on LPS-induced tubular cell stress at 6 h. NAD(P)H autofluorescence intensity was used as an indicator of tubular cell stress. Representative video images of NAD(P)H autofluorescence from a saline-treated (A), LPS-treated (10 mg/kg, i.p.) (B) and L-NIL + LPS-treated mice (C) at 6 h are shown. LPS produced a significant increase in NAD(P)H autofluorescence at 6 h (*$p < 0.05$

25

compared with Saline). Treatment with L-NIL (3 mg/kg, i.p.) blocked this effect of LPS.

Data are mean ± S.E.M. (n = 6). Magnification 200x.

Fig. 1.

Fig. 2.

A



B

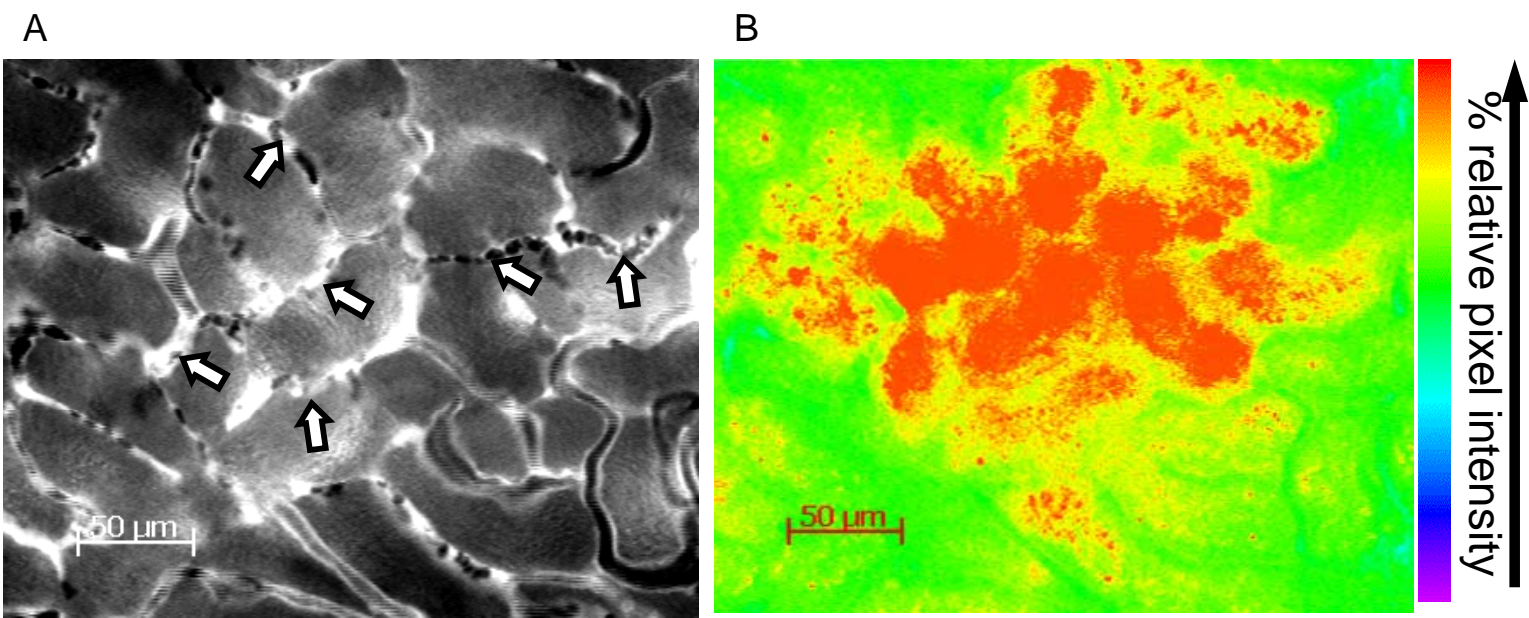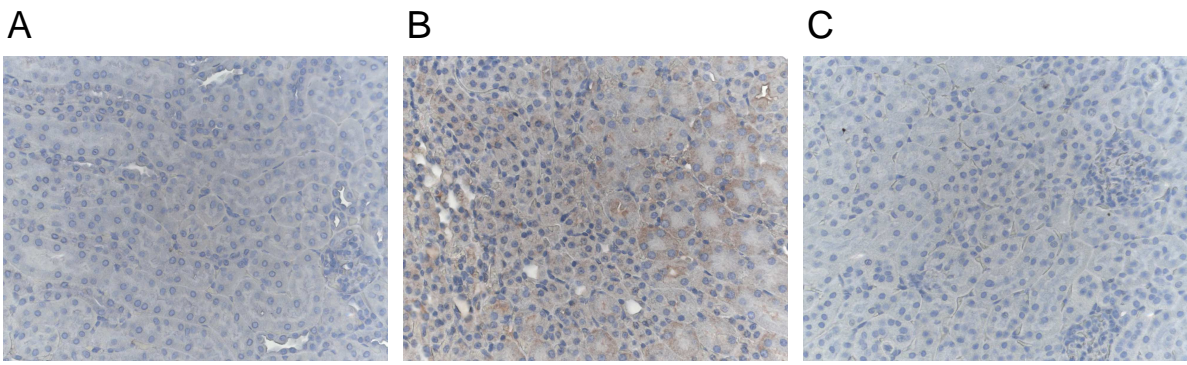

C



D

Fig. 3.

A

B



% relative pixel intensity

Fig. 4.

A

B

C

Fig. 5.



**Continuous Flow**

**Intermittent Flow**

**No Flow**

Fig. 6.

A



100 μm

B



100 μm

C



100 μm

D

Fig. 7.

A



100 µm

B



100 µm

C



100 µm

D